Desalination and Water Treatment
www.deswater.com
doi: 10.1080/19443994.2014.974216

56 (2015) 3607–3616
December

Taylor & Francis
Taylor & Francis Group

Ammonium removal by liquid–liquid membrane contactors in water purification process for hydrogen production

Edxon Licon[a,*], Mònica Reig[a], Pilar Villanova[a], Cesar Valderrama[a], Oriol Gibert[a,b], José Luis Cortina[a,b]

[a]*Chemical Engineering Dept., UPC-Barcelona TECH, Av. Diagonal 647, 08028 Barcelona, Spain, Tel. +34 934016997; emails: edxon.eduardo.licon@upc.edu (E. Licon), monica.reig@upc.edu (M. Reig), pilar.villanova@gmail.com (P. Villanova), Tel. +34 934015877; email: cesar.alberto.valderrama@upc.edu (C. Valderrama), Tel. +34 934011818; email: oriol.gibert@upc.edu (O. Gibert), Tel. +34 934016570; email: jose.luis.cortina@upc.edu (J.L. Cortina)*
[b]*CETAQUA Carretera d'Esplugues, 75, 08940 Cornellà de Llobregat, Spain*

Received 15 July 2014; Accepted 2 October 2014

ABSTRACT

In this work, a liquid–liquid membrane contactor (LLMC) was evaluated to remove ammonia traces from water used for hydrogen production by electrolysis. Three operational parameters were evaluated: the feed flow rate, the initial ammonia concentration in the water stream, and the pH of solution. Synthetic aqueous solutions with ammonium concentration of 5–25 mg L^{-1} and a sulfuric acid solution (pH 2) were supplied to the LLMC in countercurrent and open-loop configuration with flow rates between 2.72×10^{-6} and 22.6×10^{-6} m^3 s^{-1} and the pH values of the solution with ammonium between 8 and 11. A 2D numerical model was developed considering advection–diffusion equation inside a single fiber of the lumen with fully developed laminar flow and liquid–gas equilibrium in the membrane–solution interface. Predictions of the model were then validated against experimental data, which were found to be in good agreement. According to both, experimental data and numerical predictions, the hollow-fiber membrane contactor technology is a suitable alternative to remove ammonium from water and to feed the membrane distillation unit in order to fulfill water quality requirements for electrolysis-based hydrogen production.

Keywords: Ammonium removal; Membrane contactors; Open-loop configuration; Numerical simulation

1. Introduction

Hydrogen is considered a clean energy source since only water vapor is obtained during its combustion. However, its production from water by electrolysis is limited by water quality requirements in terms of ionic conductivity. This study is part of a project which had the purpose of reducing the water footprint of urban water treatment plants by coupling hydrogen generating stations. This hydrogen would be produced by

*Corresponding author.

Presented at the IX Ibero-American Congress on Membrane Science and Technology (CITEM 2014), 25–28 May 2014, Santander, Spain

electrolysis of water produced by the treatment plant. As essential requirements, the water introduced to the electrolyzer should had a low concentration of suspended solids and low conductivity [1]. For this purpose, ultrafiltration and membrane distillation units were initially installed. However, the presence of ammonia was detected in the feeding water [2].

Due to its ionic nature, the present ammonium contributes to high conductivity of the solution, decreasing the efficacy of the electrolyzer even when ammonia concentration was very low (5–15 mg L^{-1}). In turn, the fact that ammonia is a volatile compound makes difficult its elimination when water is purified using direct contact membrane distillation to remove salts and other compounds evaporating the water [3].

Ammonium is converted into ammonia at pH values higher than the pKa = 9.3 at 298 K, and its equilibrium is shown in Eq. (1).

$$[NH_4^+] + [H_2O] \leftrightarrow [NH_3]_g + [H_3O^+] \quad (1)$$

Due to this characteristic, a membrane contactor with hydrophobic membrane was proposed to remove the ammonium traces in the water. A membrane contactor is a device in which a transfer of mass from gas to liquid, liquid to liquid, or liquid to gas is produced without dispersion of one of the phases into the other [4]. For the liquid–liquid mode, the transfer of the molecules through the walls of the hollow membranes is produced by the existence of a concentration gradient between the solution inside (lumen) and the solution flowing outside the fiber (shell). The membrane enhances the transfer of molecules through the pores of the fibers and provides direct contact between the removed gas and both fluids, avoiding the mixing between the two resulting solutions [5].

The removal of ammonia by membrane distillation has been studied previously. For instance, Xie et al. [6] studied the removal of wastewater containing low levels of ammonia (100 mg L^{-1}) through simulation of experiments with sweep gas membrane distillation at pH 11.5. Ding et al. [7] compared the separation performance of three kinds of membrane distillation, direct contact membrane distillation, vacuum membrane distillation, and sweeping gas membrane distillation used in the removal of ammonia from water. They determined key factors that may affect the separation processes, such as the membrane characteristics, the feed temperature, feed and permeate velocity, and the initial concentration and pH of the feed solution. EL-Bourawi et al. [8] investigated the applicability of vacuum membrane distillation for ammonia removal from its aqueous solutions using membrane distillation was also studied by Bourawi et al. [8] obtaining removal efficiencies higher than 90%.

On the other hand, the removal mechanism of ammonium using hollow-fiber membrane contactors has been studied in the last years and a variety of mathematical models can be found. Semmens et al. [9] studied the nonlinear relation on the resistances related to the transport of ammonia. Wickramasinghe et al. [10] demonstrated that the separation efficiency was controlled by the resistance in the lumen side and determined the mass transfer coefficients of ammonia using different configurations. Tan et al. [11] modeled the removal of ammonia and compared its results with experimental work carried out with polyvinylidene fluoride membrane contactors, incorporating the resistance in the feed and membrane phases. Ashrafizadeh and Khorasani [4] studied the influence of different parameters, such as inlet feed flow, initial concentration, temperature, or pH, on the ammonia removal efficiency and optimized the process for a commercial membrane contactor. Mandowara and Bhattacharya [12] developed a 2D mathematical model for polypropylene (PP) membrane contactors incorporating the effect of pore diffusion, mass transfer resistance was taken into account. Agrahari et al. [13] developed a model incorporating molecular and Knudsen diffusion effects as well as the rates of adsorption and desorption of ammonia molecules to and from the walls of the pores during the transport through the membrane. More recently, Rezakazemi et al. [14] used a finite element approach to solve a 2D diffusion model to predict the unsteady state of ammonia transport. Nosratina et al. [15] included the continuity equation for the transport of ammonia inside the membrane pores, which was considered to be controlled by diffusion. Most of the past work has been done for close-loop configuration and only in a previous work [5], Mandowara and Bhattacharya studied the open-loop case with liquid–gas configuration working under vacuum conditions in the shell side of the contactor. Accordingly, in order to understand the phenomena occurring in the separation process studied here, it is necessary to develop a model were the open-loop liquid–liquid configuration can be described considering all contributions made by the authors previously mentioned. This configuration is more reliable in terms of the water hydrolysis process since it is desired to operate in continuous regimen at pilot-plant scale.

The present work is a feasibility study on the use of liquid–liquid membrane contactors (LLMCs) in open loop for removing traces of ammonia from water, in order to fulfill the adequate conditions for the production of hydrogen by electrolysis. The

dependence of the removal efficiency on the initial concentration, pH, and flow rate will be evaluated experimentally, and numerical simulations will be used to describe the transport phenomena in the LLMC. It will be demonstrated that the use of open-loop configuration is possible when using a given number of membrane contactors in series.

2. Material and methods

2.1. Experimental description and operation

Experiments were carried out using the setup shown in Fig. 1. It consisted of the LLMC module, two peristaltic pumps and two PP tanks, one for the ammonium chloride solutions and the other for the sulfuric acid solution at pH 2 (0.02 M). The volume of the acid solution was 25 l. All test components were connected by clear PVC flexible tubes. The contactor module used was a Liqui-Cel 2.5 × 8″ Extra Flow X30HF (Celgard, USA). The pH of the ammonium solution was increased by adding sodium hydroxide, and the solution was buffered with sodium tetraborate. All reagents used were of analysis quality (PA-ACS-ISO reagent, PANREAC). The ammonia concentration at the outlet of the module was determined during the experiments with a selective ammonia electrode (HACH 51927) with a sampling time of 5 min until the steady state was reached. The values reported are those obtained in the steady state.

The experiments were divided in three different groups in order to evaluate the performance of the process under several values of the flow rate (Q), pH of the ammonium solution, and its initial ammonium concentration (C_0). All the values are listed in Table 1.

Table 1
Values of the parameters studied for the three different groups of experiments

Experiment group	$Q \times 10^6$ ($m^3\ s^{-1}$)	pH	C_0 (mg L^{-1})
Flow rate	2.72	10	15
	3.48		
	6.12		
	8.86		
	13.3		
	22.6		
pH	3.48	8	15
		8.5	
		9	
		9.5	
		10	
		11	
Initial concentration	3.48	10	5
			10
			15
			20
			25
			35

2.2. Theory and model development

In aqueous solution, ammonium and ammonia are present depending on the pH equilibrium. This is an unsteady-state process in which the transport is governed by axial diffusion, radial diffusion, and convection in the lumen side. A three-step transport may be considered to occur sequentially during the ammonia

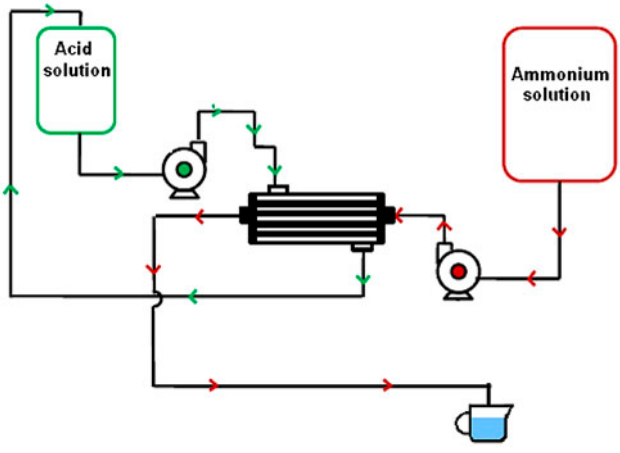

Fig. 1. Experimental setup for the study of ammonium removal in open-loop configuration with a LLMC.

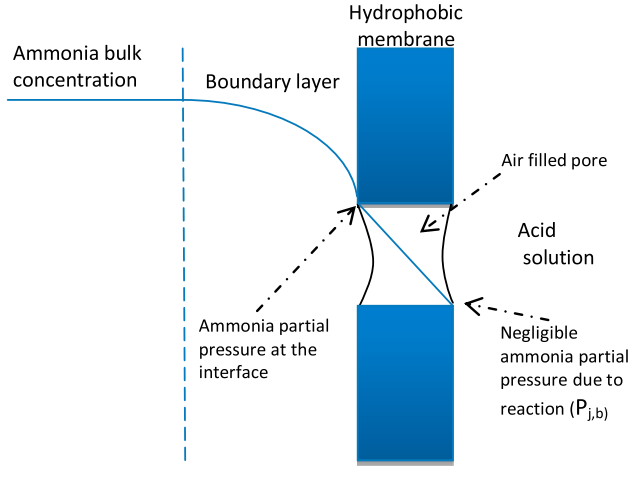

Fig. 2. Ammonia partial pressure profile when it moves from a liquid phase toward an acid solution through a hydrophobic membrane.

removal (see Fig. 2). The first step is radial diffusion to the internal surface of the hollow fiber. The second step is the diffusion of ammonia inside the pore. Finally, ammonia in gaseous form reaches the pore exit of the hydrophobic membrane and instantaneously reacts with the acid solution. No reaction zone is formed due to the high solubility of the ammonia in acid solutions; it reacts only at the interface. Given the above considerations, the numerical model is based on the following assumptions [12]:

(1) Isothermal operation;
(2) Fully developed parabolic profile in the lumen side;
(3) No pore blockages and pores are filled with air;
(4) Feed and extract volumes (and hence tank volumes) are large compared to that of the hollow-fiber module;

Let N_j be the molar flux of species j being transferred then at steady state, molar flux may be written as [16]:

$$N_j = k_{j,l}(C_{j,b} - C_{j,\text{int}}) = k_{j,g,\text{pore}}\left(\frac{p_{j,\text{int}} - p_{j,b}}{R_g T}\right) \tag{2}$$

where $k_{j,l}$, $k_{j,g,\text{pore}}$, $C_{j,\text{int}}$, $p_{j,\text{int}}$, $C_{j,b}$, $P_{j,b}$, T, and R_g denote, respectively, the mass transfer coefficient in the liquid phase for the species j, the mass transfer coefficient in the hydrophobic membrane for the species j, the interfacial gas concentration in the liquid, the partial pressure of component j at the interface, the bulk concentration of component j in the liquid, the bulk partial pressure of component j, the temperature, and the universal gas constant.

At the liquid–gas interface, Henry's law is applicable as the solution is dilute [5,11,12]:

$$P_{j\text{int}} = P^{g}_{a\text{int}} = H_a^T[\text{NH}_3]_{\text{int}} \tag{3}$$

where $H_a{}^T$ is the ammonias Henry's constant at a given temperature. Taking all this into account, the overall mass transfer coefficient ($k_{j,\text{ov}}$) is given by:

$$\frac{1}{k_{j,\text{ov}d_i}} = \frac{1}{k_{j,l}d_i} + \frac{R_g T}{H_a^T k^b_{j,g,\text{pore}}} \tag{4}$$

where negligible resistance in the permeate side is considered and the liquid mass transfer coefficient for the species j in the lumen side. The mass transport coefficient at the liquid ($k_{j,l}$) is calculated from Leveque equation under laminar flow condition [5,16]

$$K_{j,l} = 1.62\frac{D_j}{d_i}\left(\frac{d_i^2\overline{U}}{LD_j}\right)^{1/3} \tag{5}$$

Mass transfer coefficient in the hydrophobic membrane for the species j can be written as [5,12,16]:

$$k_{g,\text{pore}} = D_{a,c,\text{pore}}\left\{\frac{\varepsilon}{\tau b}\right\} \tag{5}$$

where $D_{a,c,\text{pore}}$ is the ammonia diffusivity ($\text{m}^2\,\text{s}^{-1}$), ε is porosity of the membrane, b is membrane thickness (m), and τ is tortuosity of the pore given by:

$$\tau = \frac{1}{\varepsilon^2} \tag{7}$$

In hydrophobic membranes, the pores are gas filled and the species can be transferred through the pores mainly by Knudsen or/and viscous flow depending on the ratio between the membrane pore radius and mean free path of the species. Knudsen diffusivity can be evaluated from following correlation [16]. The diffusivity of gaseous ammonia in the pore is calculated by:

$$\frac{1}{D_{a,c,\text{pore}}} = \frac{1}{D_{k,a,\text{pore}}} + \frac{1}{D_{a,\text{air}}} \tag{8}$$

where $D_{k,a,\text{pore}}$ is the Knudsen diffusion ($\text{m}^2\,\text{s}^{-1}$), $D_{a,\text{air}}$ is the ammonia diffusivity in the air ($\text{m}^2\,\text{s}^{-1}$). The Knudsen diffusion was calculated by:

$$D_{k,a,\text{pore}} = \frac{d_{\text{pore}}}{3}\left(\frac{8R_g T}{\pi M_a}\right)^{1/2} \tag{9}$$

where d_{pore} is diameter of pore (m), R_g is the universal gas constant ($\text{J mol}^{-1}\,\text{K}^{-1}$), T is the temperature (°K), and M_a is the molecular weight of ammonia (g mol^{-1}).

On the other hand, for cross-flow hollow-fiber modules (see Fig. 3), the hydraulic mean diameter (d_h) can be described as a function of the outer diameter of the central delivery tube (d_D), the shell inner diameter (d_a), and the outer fiber diameter (d_o):

$$d_h = \frac{d_a^2 - d_D^2 - Nd_o^2}{Nd_o} \tag{10}$$

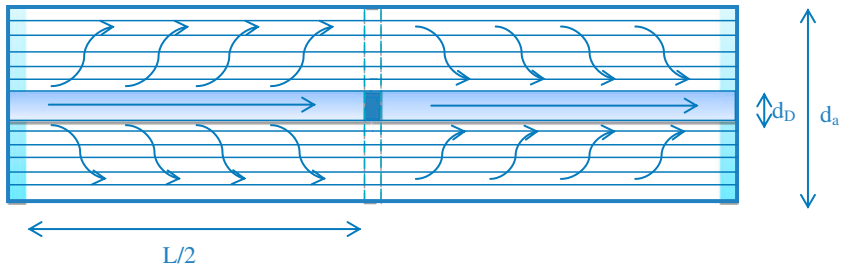

Fig. 3. The schematic view of the cross-flow hollow-fiber module with the velocity profile of flow in the shell side compartment.

For those modules, most researchers calculate the mean linear velocity (v_{sh}) considering a radial flow pattern.

$$v_{sh} = \frac{2Q\mathrm{Ln}\left(\frac{d_a}{d_D}\right)}{\pi L(d_a - d_D)} \tag{11}$$

Then, the Reynolds number in the shell side (Re_s) is defines as [17]:

$$\mathrm{Re} = \frac{v_{sh} d_h}{\eta} \tag{12}$$

Tables 2 and 3 present the ammonia properties and the hydrophobic membrane specifications, respectively.

In the removal process, there is no chemical reaction additionally to the acid–base reaction in the lumen side. The symmetry assumed inside the lumen is cylindrical. Furthermore, the radial component of velocity also becomes zero, the rate of diffusion of ammonia in water is negligible and the flow is in the Z direction. Then, the transport equation follows as:

$$\frac{\partial C_j}{\partial t} + U_z \frac{\partial C_j}{\partial z} = D_j \left[\frac{1}{r}\frac{\partial}{\partial r}\left(r\frac{\partial C_j}{\partial r}\right) + \frac{\partial^2 C_j}{\partial z^2}\right] \tag{13}$$

For the processes carried out under laminar conditions, the velocity profile in the fiber can be written as:

Table 2
Properties of ammonia at T = 298 K

Properties (j is ammonia)	Values
Henry's law constant, H_j (Pa m^3 mol^{-1})	1.62
Diffusivity in water, D_j (m^2 s^{-1})	1.76×10^{-9}
Diffusivity in air, $D_{j,air}$ (m^2 s^{-1})	1.89×10^{-5}

Table 3
Specifications of the membrane used in the contactor

Hydrophobic membrane specifications	Values
Pore diameter, d_{pore} (m)	3×10^{-8}
Thickness of the membrane, b (m)	3×10^{-5}
Porosity,	0.4
Tortuosity of pore, τ	2.25
Inner diameter of the lumen, d_i (m)	2.4×10^{-4}
Outer diameter of the lumen, d_o (m)	3×10^{-4}
Effective length of the fiber, L (m)	0.15
Number of fibers, N (m)	9,950
Shell diameter d_s (m)	0.63
Fiber bundle diameter d_a (m)	0.47
Distribution tube diameter d_D (m)	0.22

$$U_z(r) = \overline{U}\left\{1 - \left(\frac{r}{R}\right)^2\right\} \tag{14}$$

where r is radial coordinate (m) and R is radius of the fiber. Defining $\overline{U}$ as the average velocity of the fluid inside the lumen:

$$\overline{U} = \frac{Q}{N\pi R^2} \tag{15}$$

where Q is the flow rate (m^3 s^{-1}) and N is the number of fibers in the LLMC. Once defined the equations for the mass balance within fiber, the boundary conditions are defined by:

Constant concentration at the inlet of the lumen:

$$C_{j,z=0} = C_0 \tag{16}$$

The boundary condition at the exit of the lumen is defined assuming the diffusion of ammonia to be negligible in comparison with its movement in the same direction of bulk flow,

$$\left(\frac{\partial^2 C_j}{\partial r^2}\right)_{z=L} = 0 \tag{17}$$

In addition, due to the cylindrical shape of the fiber radial symmetry can be defined along its middle point as:

$$\left(\frac{\partial C_j}{\partial r}\right)_{r=0} = 0 \tag{18}$$

Finally, at the inner surface of the hollow fiber, the flux of the ammonia in aqueous phase equals the flux of the gaseous ammonia diffused through the pore [12]:

$$-D_j\left(\frac{\partial C_j}{\partial r}\right)_{r=R} = k_{g,\text{pore}}\left(\frac{p^g_{a,\text{int}}}{R_g T}\right) \tag{19}$$

where $P^g{}_{a,\text{int}}$ is the partial pressure of the ammonia at the liquid membrane interface.

The total ammonium concentration (C_j) (mol m^{-3}) in the aqueous solution is calculated by:

$$C_j = [\text{NH}_3] + [\text{NH}_4^+] \tag{20}$$

where both concentrations could be estimated using the acid dissociation constant $K_a(T)$ (NH_4^+/NH_3).

$$K_a(T) = \frac{[\text{NH}_3][\text{H}^+]}{[\text{NH}_4^+]} \tag{21}$$

On the other hand, at the liquid (feed phase)–gas (porous phase) interface, Henry's law can be applied:

$$P^g_{a\text{int}} = H^T_a[\text{NH}_3]_{\text{int}} \tag{22}$$

$P^g{}_{a\ \text{int}}$ is the partial pressure of the ammonia at the interface, H^T_a is Henry's constant (Pa m^3 mol^{-1}), and $[NH_3]_{int}$ is concentration of ammonia at liquid–gas interface (mol m^{-3}). The temperature dependence of $K_a(T)$ and H^T_a could be described by Montes et al. [18]

$$K_a(T) = 10^{0.05-2{,}788/T} \tag{23}$$

$$H^T_a = \left[\left(\frac{0.2138}{T}\right) \times 10^{6.123-1{,}825/T}\right] \times R_g T \tag{24}$$

2.3. Numerical simulation

On this study, the mass transport inside the lumen was simulated using CFD techniques based on finite element method. All the equations related to the separation process with their appropriate boundary conditions were solved using COMSOL Multiphysics version 4.2a. The equations were solved with parallel direct linear solver with a relative tolerance of 0.001. Under these conditions, the solver is well suited for solving stiff and non-stiff nonlinear boundary value problems. Adaptive mesh refinement was used to mesh one of the fibers of the LLMC. Furthermore, a refinement on the mesh near to the membrane surface was implemented for all the calculations. A Dell-PC-Intel core 2 (CPU speed is 3 GHz) was used to solve the sets of equations. The mathematical model was developed following the assumptions made by Mandowara and Bhattacharya [12] without taking into account the recirculation in the ammonium solution tank.

3. Results and discussion

3.1. pH dependence

According to Fig. 4, the ammonium removal was clearly affected by the solution's pH. The equilibrium between the ammonia gas and ammonium ions depends on the solution's pH, making it the driving force responsible for the separation process. On the same figure, it can be seen within the pH range studied that the model fits the experimental data better at low pH than to at higher. Although the model does not consider the concentration of ammonia at the shell side, it was not comparable to the acid concentration. Even in hypothetical cases of comparable concentrations, it has to be taken into account that the parameter that controls the driven force is the ammonia

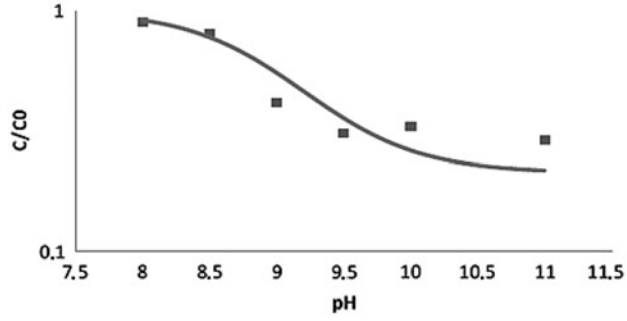

Fig. 4. Comparison between the experimental data of concentration at the outlet of the LLMC (dots) and the profile obtained numerically (line) as function of the pH.

partial pressure difference between both sides of the membrane. In order to have effects on this force, a substantial increase in the pH of the extracting solution must occur to move the ammonium equilibrium to ammonia gas, which was not the case for none of experiments carried out. Likewise, the trend predicted by the model follows qualitatively the tendency of the experimental data and moreover, a turning point is identified, which coincides with the pKa (pH 9.3), and is the reaction equilibrium between ammonium and ammonia. Two different zones are also differentiated in the plot: one for pH values below the pKa where low values of removal are obtained. The predominant species is the ammonium, and the presence of ammonia is low. The ammonia is the species that crosses the pores of the membrane and reacts with sulfuric acid resulting in ammonium sulfate, the minor presence of this species gives rise to lower elimination rates. On the other hand, at pH values above the pKa higher removal efficiencies are obtained due to the dominant presence of ammonia gas, and therefore, a greater number of molecules of the gas cross the membrane to react with sulfuric acid resulting in a higher removal performance. A further increase in the pH (>10) not represent a significant increase in ammonia removal, that should be taken into account when designing the real operational conditions in order to save reagents consumption.

3.2. Initial concentration dependence

Fig. 5 shows the results of the experimental data and for the removal of ammonium at different initial concentrations of ammonium. It can be observed that the trend of the evolution is similar for the six experiments. Nonetheless, when comparing against the profile obtained numerically, differences between them are observed. As can be seen, this error does not have a clear dependence and make think that can be related to errors inherent to the experimental determinations. Accordingly, it can be considered that the removal of ammonium is independent of the initial concentration of the solution to be treated. This is in agreement with the result presented for several authors working in liquid–liquid mode but closed loop regime [12,14,15].

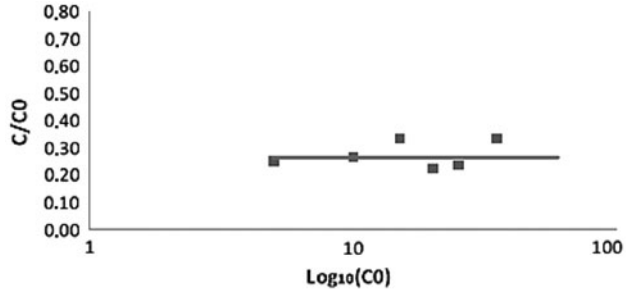

Fig. 5. Comparison between the experimental data of concentration at the outlet of the LLMC (dots) and the profile obtained numerically (line) as function of the initial concentration of ammonium, C_0 (mg L^{-1}).

3.3. Flow rate dependence

The other important parameter to be taken into account is the flow rate, which affects the residence time of the solution inside the LLMC; the larger the flow rates the lower the efficiency of the contactor (see Fig. 6). For each experiment, its respective linear velocity (U) was calculated by means of Eq. (15), and the results are presented as function of the reciprocal velocity ($1/U$).

According to Fig. 6, the model is substantially consistent with the experimental data. However, the fact that both are not identical can be attributed again to experimental error, such as the presence of any air bubbles in the circuit and the error in the ammonia selective electrode, among others. It can be seen, that at low values f of $1/U$ (at high flows) lower removal is reached. Additionally, it can be seen that the profile presents a zone in which a small change in flow results in a large variation in ammonia removal. Nevertheless, it has to be taken into account that very low flow rates may produce an extra resistance in the liquid phase.

This behavior is in concordance with the values reported in a previous work [5].

3.4. Mass transport coefficient calculation

From Eq. (4), the overall mass transport coefficient can be calculated for each flow defined in the experimental part (Table 1). Fig. 7 shows how this coefficient

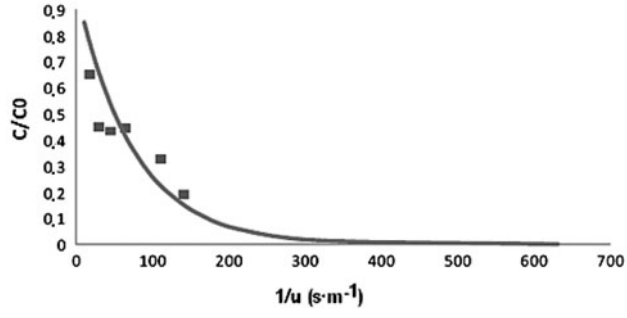

Fig. 6. Comparison between the experimental data of concentration at the outlet of the LLMC (dots) and the profile obtained numerically (line) as function of the initial concentration of ammonium, C_0 (mg L^{-1}).

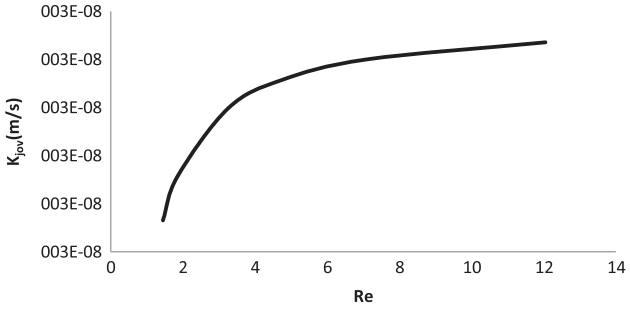

Fig. 7. Overall mass transport coefficient as function of the Reynolds number in the lumen.

is almost independent to Reynolds numbers (in the lumen) larger than 6. Nevertheless, the variation in the complete range is just about 1.5%. Calculated values of various parameters from the model equations are given in Table 4. In all the experiments, the flow can be consider laminar at both sides of the membrane due to the low values for their respective Reynolds numbers obtained with Eq. (12) (Table 5).

In order to generalize the results of this study, the following dimensionless variables are introduced:

$$\xi = \frac{2r}{d_i}; \zeta = \frac{z}{L}; \breve{C} = \frac{c}{c_0} \tag{25}$$

with the use of these new variables and after simplification at the steady state, the transport equation and its boundary conditions result in:

$$\frac{\partial \breve{C}}{\partial \zeta} = 2\left(\frac{DL}{Vd_i^2}\right)\left[\left(\frac{1}{1-\xi^2}\right)\left\{\frac{1}{\xi}\frac{\partial}{\partial \xi}\left(\xi\frac{\partial \breve{C}}{\partial \xi}\right)\right\}\right] \tag{26}$$

$$\breve{C}_{\zeta=0} = 1; \frac{\partial^2 \breve{C}}{\partial \zeta^2}_{\zeta=1} = 0; \frac{\partial \breve{C}}{\partial \xi}_{\xi=0} = 0; \frac{\partial \breve{C}}{\partial \xi}_{\xi=1} = -\frac{\mathrm{sh}}{2}\breve{C}_{\xi=1} \tag{27}$$

where the coefficient $\mathrm{sh} = \frac{k_{g,\mathrm{pored}_i}}{D_j} = 55.4$ is the Sherwood number and the term $\frac{Vd_i^2}{DL}$ is the dimensionless Graetz number based on the internal fiber diameter, which is related to the Reynolds and Schmidt numbers as $\mathrm{Gr} = \frac{\mathrm{ReScdi}}{L}$. The Sherwood number represents the ratio of convective to diffusive mass transport. According to value obtained in this study, the mass transport occurring in the boundary was carried out mainly by convective transport instead of molecular diffusion. On the other hand, when the definition of the Sherwood number is changed to $\frac{k_{g,\mathrm{pored}_i}}{D_{a,c,\mathrm{pore}}}$, the obtained value of it is lower than 1. The combined diffusivity in the pore $(D_{a,c,\mathrm{pore}})$ takes into account the effects of the Knudsen diffusion and the value near to the unity in the new definition of the Sherwood number, which means that the Knudsen diffusion is the responsible of the mass transport in the membrane pore. These results are in agreement with values reported in the literature [12] .

3.5. Number of modules

Taking into account all the results, it can be said that when the pH values promote a high concentration of ammonia and the flow rate maintains an adequate residence time, the LLMC will remove the same percentage of the ammonium from the feeding solution when working in open-loop configuration irrespective of the feed concentration.

The fraction of ammonia at the end of a single contactor can be defined as:

$$X^* = \frac{C}{C_0} \tag{28}$$

Accordingly, when placing N_m number of LLMC in series the resultant concentration can be expressed through:

$$C = C_0 X^{*Nm} \tag{29}$$

Therefore, the number of modules to be used to reach a given concentration can be calculated from such simple expression:

$$N_m = \frac{\log(\frac{C^*}{C_0})}{\log(X^*)} \tag{30}$$

where C^* is the desirable concentration.

Table 4
Calculated values of various parameters from the model equations

Parameter	Value
Mass transfer coefficient in the hydrophobic membrane for $NH_{3(g)}$, $k_{j,g,\mathrm{pore}}$ (m s^{-1})	4.06×10^{-4}
Knudsen diffusivity, $D_{k,j,\mathrm{pore}}$ (m^2 s^{-1})	1.92×10^{-7}
Combined diffusivity, $D_{j,c,\mathrm{pore}}$ (m^2 s^{-1})	1.90×10^{-7}

Table 5
Reynolds numbers in the lumen (Re) and the shell side (Re_s)

Q ($m^3\ s^{-1}$) × 10^6	Re	Re_s
2.72	1.45	2.01
3.48	1.85	2.57
6.12	3.26	4.53
8.86	4.72	6.56
1.33	7.09	9.85
2.26	12.04	16.74

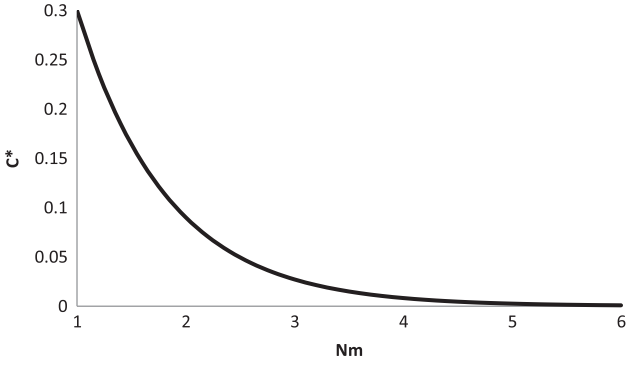

Fig. 8. Ammonia concentration at the outlet of the series of contactors as function of the number of modules.

For instance, the value of X^* obtained from experiments with pH of 10 and flow rate of feed of 3.48 × 10^{-6} $m^3\ s^{-1}$ was nearly 0.3 for experimental data. Fig. 8 shows the ammonia concentration against number of modules (N_m) in series, and it is observed that removal efficiency can be larger to 95% with three modules.

4. Conclusions

In view of the results of this study, the technology of LLMC operating in open-loop configuration is potentially suitable to remove water with low levels of ammonium. The effect of the feed stream pH, initial concentration of ammonium, and flow rate was thoroughly studied in order to describe its influence during the removal process, and it was determined a simple expression to estimate the number of membrane modules placed in series necessary to reach a given target value. The maximum efficiency experimentally observed for single step was 78% under feed values of pH, initial concentration, and flow rate of 10, 2.72×10^{-6} $m^3\ s^{-1}$ and 15 mg L^{-1}, respectively.

Furthermore, it is demonstrated experimentally and numerically that the ammonium removal efficiency in LLMC operating in open-loop configuration is improved by raising the pH and decreasing the flow rate. Accordingly, the model proposed in this study can describe properly the experimental data and can be used to evaluate and design the ammonia removal process by LLMCs.

Acknowledgments

This study has been supported by the ZERODISCHARGE project (CPQ2011-26,799) financed by "Ministerio de Economía y Competitividad" and the Catalan government (project Ref. 2009SGR905). The authors also thank to A. Gali, E. Larrotcha, and E. Marzo, project leaders of the Greenlysis project from CETAQUA, for their support and help on the study.

List of symbols

A — membrane surface area (m^2)
b — membrane thickness (m)
C^* — desirable concentration at the outlet of the modules (mol m^{-3})
C_j — the total ammonium concentration in the feed phase (mol m^{-3})
C_0 — the inlet concentration (mol m^{-3})
$D_{a,\text{air}}$ — the ammonia diffusivity in the air ($m^2\ s^{-1}$)
$D_{a,c,\text{pore}}$ — the ammonia diffusivity ($m^2\ s^{-1}$),
D_j — diffusivity of the component j in water ($m^2\ s^{-1}$)
$D_{k,a,\ \text{pore}}$ — the Knudsen diffusion ($m^2\ s^{-1}$)
d_{pore} — diameter of pore (m)
H_a^T — Henry's constant (Pa·m^3 mol^{-1})
K_a — ammonium acid dissociation constant
$K_{g,\text{pore}}$ — the mass transfer coefficient inside the pore ($m\ s^{-1}$)
L — length of the hollow fibers (m)
M_a — the molecular weight of ammonia (g mol^{-1})
N — the number of fibers in the HFMC
N_m — the number of modules
$[NH_3]$ — the concentrations of ammonia (mol m^{-3})
$[NH_{3\ (g)}]$ — the concentration of ammonia gas (mol L^{-1})
$[NH_4^+]$ — the concentrations of ammonium in the feed solution (mol m^{-3})
$P^g_{a\ \text{int}}$ — the partial pressure of the ammonia at the interface (Pa)
Q — the flow rate ($m^3\ s^{-1}$)
R — the radius of the fiber (m)
r — radial coordinate (m)
R_g — the universal gas constant (J mol^{-1} K^{-1}),
T — the temperature (K)
U — the velocity ($m\ s^{-1}$)
$\overline{U}$ — average velocity ($m\ s^{-1}$)
V — volume (m^3)
X^* — fraction obtained with one module
z — axial coordinate (m)
ε — porosity of the membrane,
τ — tortuosity

References

[1] A. Ursua, L.M. Gandia, P. Sanchis, Hydrogen production from water electrolysis: Current status and future trends, Proc. IEEE. 100 (2012) 410–426.

[2] E. Marzo, A. Gali, B. Lefevre, L. Bouchy, A. Vidal, J.L. Cortina, A. Fabre, Hydrogen and oxygen production using wastewater effluent treated with ultra-filtration and membrane distillation (greenlysis), Procedia Eng. 44 (2012) 1744–1746.

[3] P. Peng, A.G. Fane, X. Li, Desalination by membrane distillation adopting a hydrophilic membrane, Desalination 173 (2005) 45–54.

[4] S.N. Ashrafizadeh, Z. Khorasani, Ammonia removal from aqueous solutions using hollow-fiber membrane contactors, Chem. Eng. J. 162 (2010) 242–249.

[5] A. Mandowara, P.K. Bhattacharya, Membrane contactor as degasser operated under vacuum for ammonia removal from water: A numerical simulation of mass transfer under laminar flow conditions, Comput. Chem. Eng. 33 (2009) 1123–1131.

[6] Z. Xie, T. Duong, M. Hoang, C. Nguyen, B. Bolto, Ammonia removal by sweep gas membrane distillation, Water Res. 43 (2009) 1693–1699.

[7] Z. Ding, L. Liu, Z. Li, R. Ma, Z. Yang, Experimental study of ammonia removal from water by membrane distillation (MD): The comparison of three configurations, J. Memb. Sci. 286 (2006) 93–103.

[8] M.S. EL-Bourawi, M. Khayet, R. Ma, Z. Ding, Z. Li, X. Zhang, Application of vacuum membrane distillation for ammonia removal, J. Memb. Sci. 301 (2007) 200–209.

[9] M.J. Semmens, D.M. Foster, E.L. Cussler, Ammonia removal from water using microporous hollow fibers, J. Memb. Sci. 51 (1990) 127–140.

[10] S.R. Wickramasinghe, M.J. Semmens, E.L. Cussler, Mass transfer in various hollow fiber geometries, J. Memb. Sci. 69 (1992) 235–250.

[11] X. Tan, S.P. Tan, W.K. Teo, K. Li, Polyvinylidene fluoride (PVDF) hollow fibre membranes for ammonia removal from water, J. Memb. Sci. 271 (2006) 59–68.

[12] A. Mandowara, P.K. Bhattacharya, Simulation studies of ammonia removal from water in a membrane contactor under liquid–liquid extraction mode, J. Environ. Manage. 92 (2011) 121–130.

[13] G.K. Agrahari, S.K. Shukla, N. Verma, P.K. Bhattacharya, Model prediction and experimental studies on the removal of dissolved NH_3 from water applying hollow fiber membrane contactor, J. Memb. Sci. 390–391 (2012) 164–174.

[14] M. Rezakazemi, S. Shirazian, S.N. Ashrafizadeh, Simulation of ammonia removal from industrial wastewater streams by means of a hollow-fiber membrane contactor, Desalination 285 (2012) 383–392.

[15] F. Nosratinia, M. Ghadiri, H. Ghahremani, Mathematical modeling and numerical simulation of ammonia removal from wastewaters using membrane contactors, J. Ind. Eng, Chem. 20(5) (2013) 2958–2963.

[16] E. Drioli, A. Criscuoli, E. Curcio, Membrane contactors: Fundamentals, applications and potentialities, Elsevier, Amsterdam, 2006.

[17] S. Shen, S.E. Kentish, G.W. Stevens, Shell-side mass-transfer performance in hollow-fiber membrane contactors, Solvent Extr. Ion Exch. 28 (2010) 817–844.

[18] F. Montes, C.A. Rotz, H. Chaoui, Process modeling of ammonia volatilization from ammonium solution and manure surfaces: A review with recommended models, Trans. Asabe. 52 (2009) 1707–1719.